Article

Cell Reports

DNA Topology and Global Architecture of Point Centromeres

Graphical Abstract

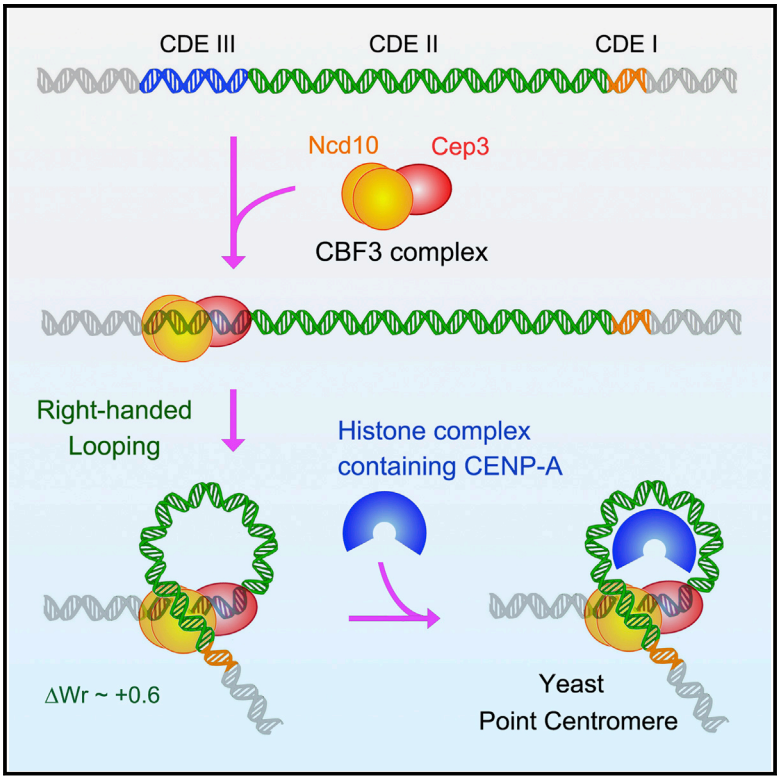

Highlights

- Point centromeres increase the ΔLk of DNA by +0.6 units in yeast minichromosomes
- This ΔLk change is constrained by the topology of CDEs within the point centromere
- Centromere DNA topology is independent of CDEII length and of cbf1 binding to CDEI
- Constraining of ΔLk +0.6 is established by the integrity of CDEII and CDEIII

Authors

Ofelia Díaz-Ingelmo, Belén Martínez-García, Joana Segura, Antonio Valdés, Joaquim Roca

Correspondence

joaquim.roca@ibmb.csic.es

In Brief

Díaz-Ingelmo et al. show that the point centromere of budding yeast constrains a positive DNA supercoil, which requires the centromere DNA elements CDEII and CDEIII, but not CDEI. This positive supercoil suffices to accommodate a sub-octameric histone complex, which does not have to be inherently right-handed.

Díaz-Ingelmo et al., 2015, Cell Reports *13*, 667–677
October 27, 2015
http://dx.doi.org/10.1016/j.celrep.2015.09.039

Cell Reports
Article

DNA Topology and Global Architecture of Point Centromeres

Ofelia Díaz-Ingelmo,[1] Belén Martínez-García,[1] Joana Segura,[1] Antonio Valdés,[1] and Joaquim Roca[1,*]
[1]Molecular Biology Institute of Barcelona (IBMB), Spanish National Research Council (CSIC), Barcelona 08028, Spain
*Correspondence: joaquim.roca@ibmb.csic.es
http://dx.doi.org/10.1016/j.celrep.2015.09.039

SUMMARY

DNA is wrapped in a left-handed fashion around histone octasomes containing the centromeric histone H3 variant CENP-A. However, DNA topology studies have suggested that DNA is wrapped in a right-handed manner around the CENP-A nucleosome that occupies the yeast point centromere. Here, we determine the DNA linking number difference (*ΔLk*) stabilized by the yeast centromere and the contribution of the centromere determining elements (CDEI, CDEII, and CDEIII). We show that the intrinsic architecture of the yeast centromere stabilizes +0.6 units of *ΔLk*. This topology depends on the integrity of CDEII and CDEIII, but it is independent of cbf1 binding to CDEI and of the variable length of CDEII. These findings suggest that the interaction of the CBF3 complex with CDEIII and a distal CDEII segment configures a right-handed DNA loop that excludes CDEI. This loop is then occupied by a CENP-A histone complex, which does not have to be inherently right-handed.

INTRODUCTION

The centromere is the genetic locus that organizes the kinetochore, the multi-protein complex that attaches each chromosome to spindle microtubules during mitosis and meiosis (Biggins, 2013; Bloom, 2014). In contrast to most eukaryotic centromeres that are epigenetically defined and span large domains of heterochromatin (Black et al., 2010; Henikoff and Furuyama, 2010; Burrack and Berman, 2012), the centromere of budding yeast is a compact structure occupying ~200 bp of DNA (Bloom and Carbon, 1982) and is genetically defined by three conserved centromere-determining elements (CDEs): an 8-bp palindrome called CDEI, a 26-bp sequence called CDEIII, and a 78- to 86-bp stretch of AT-rich (~90%) DNA called CDEII that lies in between (Clarke, 1998). Despite these differences in size and locus definition, all eukaryotic centromeres have a common protein determinant, namely, the histone H3 variant CENP-A (also known as Cid in *Drosophila* and Cse4 in budding yeast). Most eukaryotic centromeres thus comprise hundreds of nucleosomes that contain CENP-A (Schueler and Sullivan, 2006), whereas budding yeast contains fewer CENP-A nucleosomes (Haase et al., 2013), including a single CENP-A nucleosome positioned on the CDEs (Furuyama and Biggins, 2007; Cole et al., 2011; Krassovsky et al., 2012).

Although CENP-A nucleosomes are essential for kinetochore formation, their functional properties are unknown. Numerous lines of evidence indicate that their structure differs from canonical nucleosomes. Regarding their histone composition and CENP-A copy number, several mutually exclusive structures have been proposed. These models include conventional $(CENP\text{-}A/H4/H2B/H2A)_2$ octasomes (Camahort et al., 2009; Zhang et al., 2012; Padeganeh et al., 2013; Wisniewski et al., 2014), asymmetric $(CENP\text{-}A/H3/(H4/H2B/H2A)_2$ octasomes (Lochmann and Ivanov, 2012), $(CENP\text{-}A/H4/Scm3)_2$ hexasomes (Mizuguchi et al., 2007), $(CENP\text{-}A/H4)_2$ tetrasomes (Xiao et al., 2011; Aravamudhan et al., 2013), and CENP-A/H4/H2B/H2A hemisomes (Henikoff and Furuyama, 2012; Furuyama et al., 2013). Regarding their morphology, atomic force microscopy (AFM) studies showed that in-vitro-assembled CENP-A nucleosomes have a reduced height (Dalal et al., 2007; Dimitriadis et al., 2010; Bui et al., 2012), which is established by the CATD domain of CENP-A (Miell et al., 2013). At the point centromere of budding yeast, a histone complex containing CENP-A interacts with CDEII and is flanked by the proteins that bind to CDEI and CDEIII (Krassovsky et al., 2012). CDEI is occupied by the general transcription factor Cbf1(p39), which is not essential for centromere function (Cai and Davis, 1989; Baker et al., 1989). CDEIII is occupied by the CBF3 complex, which contains four essential proteins, namely, a Cep3 (p64) homodimer, an Skp1(p19)-Ctf13(p58) heterodimer, and an Ndc10 (p110) homodimer (Jiang et al., 1993; Lechner and Carbon, 1991; Connelly and Hieter, 1996). The observation of physical interactions between CBF3 and Cbf1 (Hemmerich et al., 2000) has led to the proposal that CDEI and CDEIII are bridged to hold a CDEII loop that stabilizes the CENP-A nucleosome (Xiao et al., 2011; Cho and Harrison, 2011).

A second striking feature of centromeric nucleosomes regards their DNA topology. Early studies described that, in yeast, circular minichromosomes with and without a centromere have unequal distributions of DNA topoisomers (Bloom et al., 1983, 1984). More recent analyses revealed that in vitro chromatin assembly with CENP-A/H4/H2B/H2A and the histone chaperone RbAp48 from *Drosophila* tends to constrain positive DNA supercoils, in contrast to the negative supercoils stabilized by conventional nucleosomes (Furuyama and Henikoff, 2009). The same study showed that the presence of a point centromere instead of a regular nucleosome in yeast circular minichromosomes

leads to a difference of approximately +2 units in the linking number of DNA (*Lk*). A similar *Lk* deviation was observed with the partitioning locus of the yeast 2-μm plasmid, which also includes a CENP-A nucleosome (Huang et al., 2011). On the basis of these observations, it was postulated that DNA wraps in a right-handed orientation in CENP-A nucleosomes (Furuyama and Henikoff, 2009; Henikoff and Furuyama, 2012). However, crystal and biochemical studies of CENP-A nucleosomes reconstituted in vitro demonstrate that they are left-handed and restrain negative DNA supercoils in a similar way to canonical octasomes (Sekulic et al., 2010; Tachiwana et al., 2011). This inconsistency has been exploited to support the notion that CENP-A nucleosomes are not left-handed octasomes (Henikoff and Furuyama, 2012). However, there is no experimental evidence of inherently right-handed histone complexes. The *Lk* differences observed in yeast centromeric minichromosomes could be explained by other protein-DNA interactions (Mishra et al., 2013) or caused by alterations of DNA topology outside the point centromere, induced either in vivo or during experimental manipulation.

Here, we analyzed the topology of DNA at the point centromere of budding yeast. Unlike previous studies that directly compared the *Lk* of circular minichromosomes with and without a functional centromere, we fixed the *Lk* of the minichromosomes in vivo (Lk^{ch}) and determined their exact *Lk* difference relative to relaxed DNA circles (Lk°). Next, we minimized the chromatin structure of the minichromosomes to discern whether the *Lk* deviations were constrained by the point centromeres or were instead due to alterations of the adjacent chromatin. Finally, we examined the contribution of CDEs in determining centromere DNA topology. Our results revealed that the intrinsic architecture of the point centromere stabilizes an *Lk* difference of +0.6 and that this topology is configured by the protein complexes bound to CDEIII and CDEII, but not to CDEI. These findings support a model of the point centromere in which the CBF3 complex configures a right-handed loop of DNA that includes the CDEIII and CDEII segments. This loop is then occupied by a CENP-A histone complex, which does not have to be innately right-handed.

RESULTS

The DNA Linking Number Difference in the Yeast TA1 Minichromosome

Circularization of the EcoRI 1,453-bp genomic fragment of *Saccharomyces cerevisiae,* which comprises the TRP1 gene and the ARS1 origin, generates a minichromosome (TA1), which replicates and segregates as a multicopy episome in *trp1* yeast strains (Thoma et al., 1984). TA1 maintains the nucleosome organization of the genomic loci (Thoma et al., 1984; Jiang and Pugh, 2009). Four nucleosomes (I–IV) are positioned downstream of the transcription start site of TRP1 and three nucleosomes (V–VII) downstream of the ARS1 region. We performed micrococcal nuclease digestions to confirm that the positions of these seven nucleosome are preserved in the TA1 minichromosome of our yeast cells (Figures 1A and S1).

As eukaryotic nucleosomes constrain negative DNA supercoils, the DNA linking number of circular minichromosomes (Lk^{ch}) is reduced with respect to that of relaxed DNA (Lk°) by a value that roughly correlates with the number of nucleosomes assembled (Prunell, 1998). For the purpose of our study, we sought to accurately determine the *Lk* difference ($\Delta Lk = Lk^{\circ} - Lk^{ch}$) of TA1. Since Lk° changes with temperature (Depew and Wang, 1975), we relaxed naked DNA circles at the same temperature that the yeast cultures. Likewise, since Lk^{ch} depends also on temperature and it can be altered by endogenous topoisomerases during cell disruption and DNA extraction, we fixed the in vivo Lk^{ch} values by quenching the yeast cultures with a cold (−20°C) ethanol-toluene solution. This fixation step irreversibly inactivates the cellular topoisomerases, so precluding the alteration of the in vivo Lk^{ch} values in subsequent manipulations (Figure S2).

Following the above considerations, we examined by gel electrophoresis the *Lk* distributions of TA1 fixed in vivo at 26°C and that of the naked TA1 circle relaxed in vitro at 26°C. In order to resolve the topoisomers of both *Lk* distributions in a single one-dimensional gel, we adjusted the concentration of chloroquine to 0.2 μg/ml during electrophoresis (Figure 1B). Otherwise, in absence of chloroquine, the *Lk* distribution of the negatively supercoiled DNA extracted from the minichromosomes would be collapsed in a fast-migration band and the *Lk* distribution of the relaxed DNA would overlap with the nicked circles (Figure S3). We examined also the same DNA samples in a two-dimensional gel along with a marker of *Lk* topoisomers, in order to unambiguously count the number of *Lk* topoisomers that separate both *Lk* distributions (Figure 1C). After counting the topoisomer bands and quantifying their individual intensities, we calculated ΔLk as the distance (*Lk* units) between the midpoints of the two distributions (Lk° and Lk^{ch}). Measurements in four independent yeast cultures indicated that TA1 has an in vivo $\Delta Lk = -9.4$ (Figure 1D).

Next, we sought to discern whether the ΔLk of TA1 was constrained by its chromatin structure. For this purpose, we cultured the same yeast cells skipping the fixation step and lysed them in order to solubilize TA1. We added a negatively supercoiled plasmid (internal DNA control) and catalytic amounts of topoisomerases (vaccinia virus topoisomerase [topo] I and *S. cerevisiae* topoisomerase II) to the lysate. We incubated the mixtures at 26°C to allow relaxation of free DNA supercoils. Electrophoretic analyses of these samples revealed that the *Lk* distribution of the solubilized TA1 minichromosomes was nearly identical to that of samples fixed in vivo and that it was not appreciably altered after incubation with topoisomerase I or topoisomerase II (Figure 1E, top). Conversely, the control plasmid included in the reactions became near fully relaxed by the endogenous topoisomerases present in the yeast lysate and completely relaxed following the addition of topoisomerase I or topoisomerase II (Figure 1E, bottom). This result indicated that the −9.4 units of ΔLk in the TA1 minichromosome are stably constrained by its chromatin structure.

A Point Centromere Deviates the *Lk* Difference of Circular Minichromosomes by +0.6 Units

Having established that TA1 stabilizes a ΔLk of −9.4, we examined how this ΔLk was modified after inserting additional chromatin elements into the minichromosome. All these experiments, including the in vivo fixation of *Lk* values, the incubation of

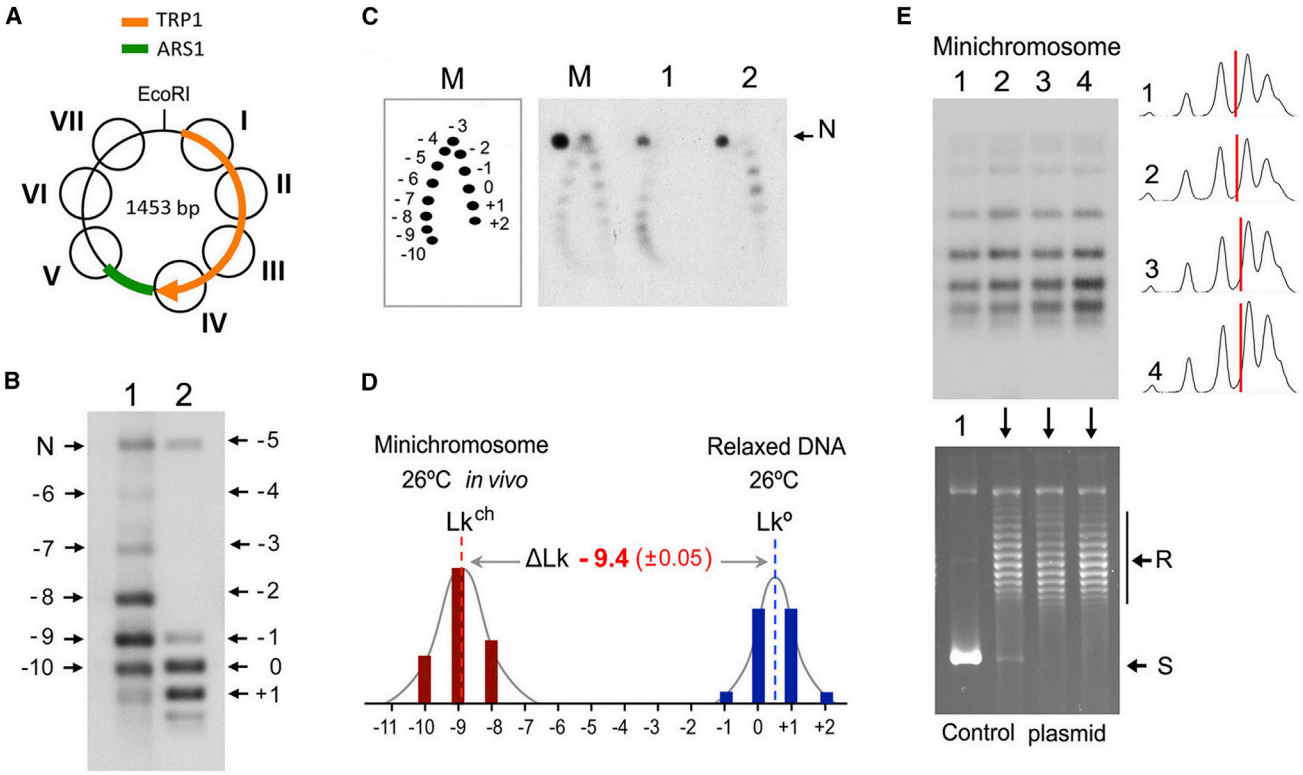

Figure 1. DNA Linking Number Difference in the Yeast TA1 Minichromosome

(A) Scheme of the TA1 minichromosome indicating the EcoRI circularization site and the position of nucleosomes I to VII with respect to the TRP1 gene and ARS1 region as determined by Thoma et al. (1984) and confirmed in the present study (see also Figure S1).

(B) One-dimensional gel electrophoresis of the distribution of *Lk* topoisomers of the TA1 minichromosome fixed in vivo at 26°C (lane 1) and of the naked TA1 circle relaxed in vitro with topoisomerase I at 26°C (lane 2). Electrophoresis was in the presence of 0.2 μg/ml chloroquine as explained in Figure S3.

(C) Two-dimensional gel electrophoresis of the same DNA samples (lanes 1 and 2) with a marker of *Lk* topoisomers (lane M). In both one- and two-dimensional gels (B and C), individual *Lk* topoisomers are identified by correlative numbers (not *Lk* values) starting with 0 at the main topoisomer of the relaxed DNA and decreasing toward the minichromosome DNA. N, nicked circles.

(D) Histogram of the signal intensity of individual *Lk* topoisomers displayed in the above gel blots. The *ΔLk* of the minichromosome is the distance (*Lk* units) between the midpoint of the in vivo *Lk* distribution (Lk^{ch}) and the midpoint of the *Lk* distribution of the relaxed DNA (Lk°). The mean *ΔLk* (±SD) of four independent experiments is indicated.

(E) The gel on the top compares the *Lk* distributions of the TA1 minichromosome extracted from fixed cells at 26°C (lane 1), solubilized in cell lysates at 26°C (lane 2), and after incubation with topoisomerase I (lane 3) or topoisomerase II (lane 4). Plots of the gel lanes and the center of intensities are shown. The gel on the bottom shows the topology of the negatively supercoiled plasmid (lane 1) that was added in excess to the above incubations (lanes 2, 3, and 4) as internal control for the relaxation activity of topoisomerases. S, supercoiled forms. R, relaxed *Lk* distribution.

solubilized minichromosomes, and the relaxation of naked DNA, were done at the same temperature (26°C). We compared the effect of three inserts, which contained the following: the positioning sequence of the nucleosome *High2* of *S. cerevisiae* (Segal et al., 2006), the point centromere of yeast chromosome IV (*CEN4*), and *CEN4* with a mutated CDEIII sequence that precludes centromere assembly (*mutCEN*) (Jehn et al., 1991). The three inserts were of identical length and were located upstream of the TRP1 gene (between nucleosomes I and VII). The result was three circular minichromosomes of 1686 bp (Figures 2A and S4).

As expected, upon yeast transformation, minichromosomes with the functional *CEN4* centromere were recovered in low copy number with respect to those with the *High2* and *mutCEN* inserts, which were recovered as high-copy episomes. As for TA1, we fixed the topology of these minichromosomes in vivo, examined their *Lk* distributions in one- and two-dimensional gels (Figure 2B), and calculated their *ΔLk* with respect to relaxed DNA circles of 1,686 bp (Figure 2C). We found that the minichromosome with the *High2* insert had a *ΔLk* of −10.8. This value implied a gain of −1.4 *Lk* units relative to TA1 and was thus compatible with the assembly of *High2* and other protein-DNA complexes at the inserted segment. Likewise, the minichromosome containing *mutCEN* had a *ΔLk* of −10.6, a gain of −1.2 *Lk* units relative to TA1, which also fitted the assembly of at least one additional nucleosome. Conversely, the minichromosome with *CEN4* presented a *ΔLk* of −8.8. This value implied a gain of +0.6 *Lk* units relative to TA1 and of +2 *Lk* units with respect to the minichromosome with the *High2* insert. This *Lk* change was incompatible with the accommodation of a left-handed nucleosomal particle at the *CEN4* sequence, unless other regions of the minichromosome had markedly altered their DNA

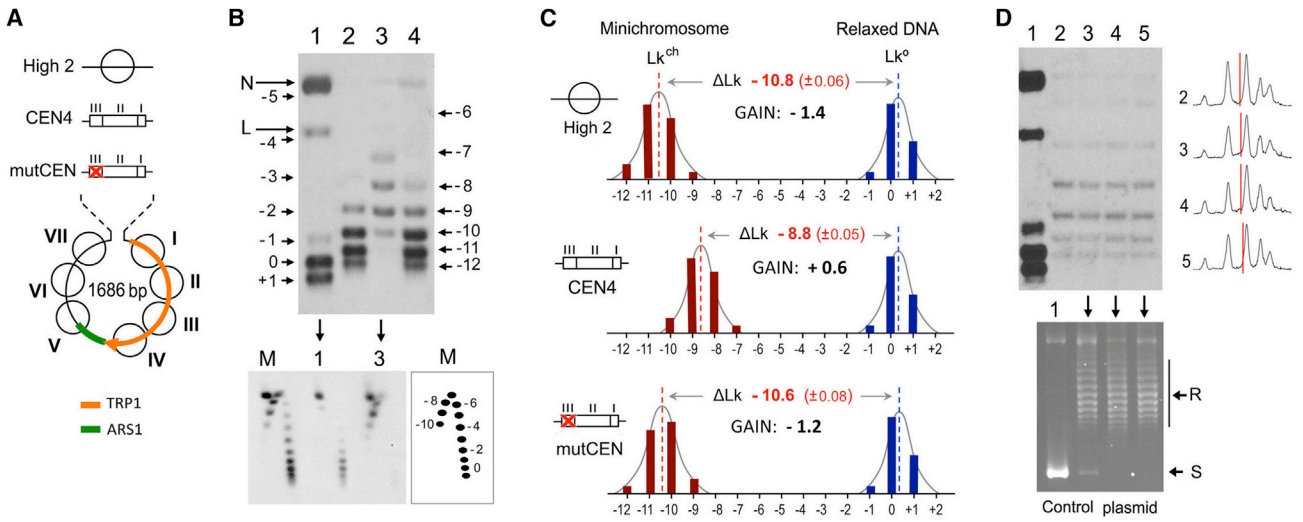

Figure 2. *Lk* Differences of Centromeric and Non-centromeric Minichromosomes of 1,686 bp

(A) Scheme of the minichromosomes of 1686 bp that were generated following the insertion of the *High2*, *CEN4*, and *mutCEN* sequences in-between the nucleosomes I and VII of TA1. See Figure S4 for details. The orientation of CDEs of *CEN4* is indicated (I, II, and III).

(B) The gel-blot on top shows the *Lk* distributions of 1,686-bp DNA circles relaxed at 26°C (lane 1), and of 1686 bp minichromosomes fixed in vivo at 26°C and that contained the *High2* (lane 2), *CEN4* (lane 3), and *mutCEN* (lane 4) inserts. One-dimensional electrophoresis was done as in Figure 1B. N, nicked circles. L, linearized circles. The two-dimensional gel (bottom) shows the *Lk* distributions of the same samples of relaxed DNA (lane 1) and of the *CEN4* minichromosome (lane 3) with a marker of *Lk* topoisomers (lane M). In both gel blots, individual *Lk* topoisomers are identified by correlative numbers.

(C) Aligned histograms of the *Lk* distributions of minichromosomes with the *High2*, *CEN4*, and *mutCEN* inserts and of the relaxed DNA circles. *ΔLk* values were calculated as in Figure 1. The mean *ΔLk* (±SD) from three independent experiments is indicated. The gain value produced by each insert is the *ΔΔLk* with respect to the *ΔLk* of the TA1 minichromosome (ΔLk −9.4).

(D) *Lk* distributions of the relaxed CEN4 DNA circle (lane 1) and of the CEN4 minichromosome fixed in vivo at 26°C (lane 2), solubilized at 26°C (lane 3), and incubated with topoisomerase I (lane 4) and topoisomerase II (lane 5). Plots of lanes 2–5 are shown. The gel on the bottom shows the control plasmid (lane 1) after its incubation with the minichromosomes of lanes 3, 4, and 5. S, supercoiled forms. R, relaxed *Lk* distribution.

topology. The *ΔLk* of the CEN4 minichromosome remained unchanged when the chromatin was solubilized and incubated with topoisomerase I or topoisomerase II (Figure 2D). Therefore, the gain of +0.6 *Lk* units induced by *CEN4* was stably constrained by the minichromosome structure.

The Gain of +0.6 *Lk* Units Is an Intrinsic Trait of the Point Centromere Architecture

The gain of +0.6 *Lk* units observed in the CEN4 minichromosomes may be stabilized by the architecture of the point centromere, but may also result from alterations of DNA topology in neighboring regions. To distinguish these two scenarios, we constructed a new set of TA1-derived minichromosomes in which we minimized the chromatin structure and the distance between functional elements (Figures 3A and S5). First, we removed nucleosomes VI and VII of TA1. We maintain nucleosome V as it partially overlaps with the ARS1 region, and we kept a minimal promoter upstream of the transcription start site of TRP1 at the 5′ flank of nucleosome I. Next, we inserted the *High2*, *CEN4*, and *mutCEN* sequences as narrowly as possible in-between nucleosomes I and V, but without interfering with the TRP1 and ARS1 functions. The result was a set of stable circular minichromosomes of 1,286 bp, in which the positioning sequence of *High2* was 39 bp from the edge of nucleosome V and 67 bp from the transcription start site of TRP1. In the case of the centromere, we allocated the CDEs of *CEN4* (111 bp) in both orientations. The centromere was functional when CDEI was 48 bp from the edge of nucleosome V and CDEIII was 93 bp from the TRP1 start site. In the reverse orientation, the centromere was functional when CDEIII was 68 bp from the edge of nucleosome V and CDEI was 73 bp from the TRP1 start site. We performed micrococcal nuclease digestions, which confirmed that the assembly of the centromere in the 1,286-bp minichromosomes did not induce loss of the flanking nucleosomes (Figure 3B). We did not obtain transformants with constructs including shorter linker regions, possibly because centromere assembly interfered with ARS1 or TRP1 functions.

We examined then the in vivo *Lk* distributions of the above 1,286-bp minichromosomes fixed in vivo (Figure 3C) and after their incubation with topoisomerases (Figure 3D). The topology of the minichromosomes was not affected by topoisomerases, which denoted that their in vivo *ΔLk* was stabilized by chromatin structure. With respect to relaxed DNA of the same length, the minichromosomes with the *High2* and *mutCEN* inserts presented a *ΔLk* of −8.2 and −8.0, respectively, whereas the minichromosomes with *CEN4* inserted in either orientation presented a *ΔLk* of −6.2 (Figure 3E). Interestingly, all these *ΔLk* values (−8.2, −8.0, and −6.2) differed by 2.6 units from the *ΔLk* values of the minichromosomes of 1,686 bp harboring the corresponding *High2*, *mutCEN*, and *CEN4* inserts (−10.8, −10.6, and −8.8). This decrease in *ΔLk* was consistent with the loss of the negative DNA supercoils that were constrained by nucleosomes VI and VII

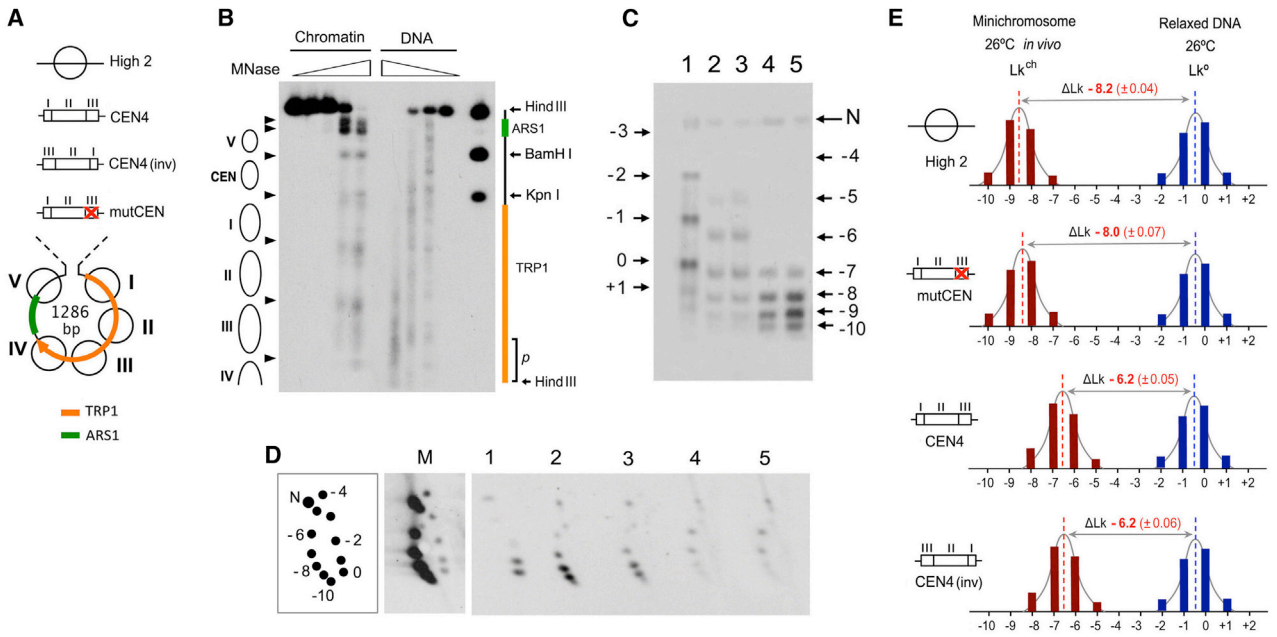

Figure 3. *Lk* Differences of Centromeric and Non-centromeric Minichromosomes of 1,286 bp

(A) Scheme of the minichromosomes of 1286 bp that were generated following the insertion of the *High2*, *CEN4*, *CEN4(inv)*, and *mutCEN* sequences closely in between nucleosomes I and V of TA1. See Figure S5 for details.

(B) Micrococcal nuclease digestion patterns of 1,286-bp minichromosomes carrying *CEN4* (chromatin) compared to naked DNA molecules (DNA). Samples digested with increasing nuclease were cut with endonuclease *Hind*III, separated on a 1.2% agarose gel, blotted, and probed with a 130-bp sequence (*p*) at the edge of the *Hind*III site.

(C) One-dimensional gel-blot comparing the *Lk* distributions of 1,286-bp DNA circles relaxed at 26°C (lane 1), and of 1286-bp minichromosomes fixed in vivo at 26°C and that contained *CEN4* (lane 2), *CEN4(inv)* (lane 3), *mutCEN* (lane 4), and *High2* (lane 5). Electrophoresis was done as in Figure 1B. N, nicked circles.

(D) Two-dimensional gel blot comparing a marker of *Lk* topoisomers (lane M) and the *Lk* distributions of 1,286-bp DNA circles relaxed at 26°C (lane 1) and of 1,286 bp minichromosomes containing *High2* (lane 2), *mutCEN* (lane 3), *CEN4* (lane 4), and *CEN4(inv)* (lane 5) following their solubilization in the presence of topoisomerase activity. N, nicked circles. In both gel blots (C and D), individual *Lk* topoisomers are identified by correlative numbers.

(E) Aligned histograms of the *Lk* distributions of the 1,286-bp minichromosomes and relaxed DNA circles. *ΔLk* values were calculated as in Figure 1D. Average values (±SD) of three independent experiments are indicated.

or nearby complexes. However, this common change of 2.6 *Lk* units also suggested that the topology of DNA in the remaining nucleosomes (I to V) was very similar in the 1,686-bp and 1,286-bp minichromosomes regardless of the elements inserted. Therefore, the gain of +0.6 *Lk* units observed in centromeric minichromosomes most likely reflects a trait of the CEN DNA topology rather than an alteration of neighboring chromatin.

The Topology of DNA at Point Centromeres Is Independent of the Length of CDEII and Is Not Altered by the Disruption of CDEI

Current models of the yeast point centromere postulate that DNA wraps around a histone core such that CDEI and CDEIII come in close proximity, and that bridging interactions between cbf1 and CBF3 then stabilize the global complex (Hemmerich et al., 2000; Xiao et al., 2011; Cho and Harrison, 2011). However, the rotational phasing between CDEI and CDEIII is not conserved in the 16 yeast centromeres due to the variable length of CDEII (from 77 to 86 bp). Then, if CDEI and CDEIII were bridged by protein interactions, the intervening CDEII segment would have to untwist or over-twist up to about half a turn (±0.5 *Lk* units) in some cases (Figure 4A). Consequently, the *ΔLk* values stabilized by point centromeres would depend on the length of CDEII. We tested this hypothesis by comparing the topology of 1,286-bp minichromosomes that carried *CEN4, CEN2, CEN7*, and *CEN12*, which have CDEII sequences of 77, 83, 85, and 86 bp, respectively (Figures 4B and S5). We found that the four centromeres produced identical *Lk* distributions (Figure 4B), in sharp contrast to the distinct helical compensations (*ΔΔLk* relative to *CEN4*) that would be required to bridge their CDEI and CDEIII elements (Figure 4C). Therefore, the stabilization of +0.6 *Lk* units by the point centromere occurs irrespective of the length of CDEII.

Since CDEI is not essential for centromere function, we questioned then whether disruption of CDEI would affect the topology of the point centromere. For this purpose, we mutated 6 bp of the CDEI sequence of *CEN4* in the 1,286-bp minichromosome to abolish its recognition by cbf1 (Wilmen et al., 1994) (Figure 5A and S5). The *ΔCDEI* minichromosome presented mitotic stability and low copy number, which corroborated that CDEI disruption does not preclude centromere function. The *ΔCDEI* minichromosome presented a $\Delta Lk = -6.2$, the same that of the *CEN4* minichromosome (Figures 5B and 5C). Therefore, the stabilization of +0.6 *Lk* units by point

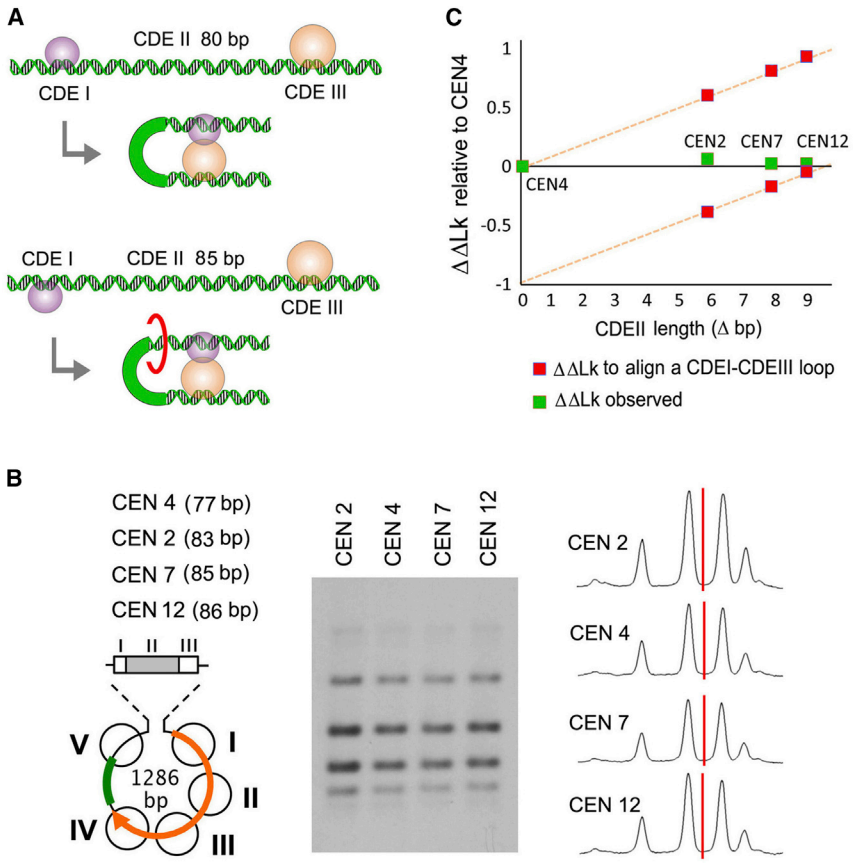

Figure 4. Effect of CDEII Length on the Topology of DNA at Point Centromeres

(A) The variable length of CDEII (e.g., 80 versus 85 bp) changes the rotational phases between CDEI and CDEIII. Bridging the proteins bound to CDEI and CDEIII would require an adjustment of the helical repeat of the intervening loop of DNA.

(B) Structure and *Lk* distributions of 1,286-bp minichromosomes that carried CEN2, CEN4, CEN7, and CEN12. The length of their corresponding CDEII element is indicated (bp). See Figure S5 for details. Electrophoresis was done as in Figure 3C. Plots of the gel lanes and the intensity center of *Lk* distribution are shown.

(C) Helical compensations (by untwisting or overtwisting) required to align CDEI and CDEIII elements as a function of CDEII length in CEN2, CEN4, CEN7, and CEN12. Theoretical values (red) are expressed as ΔΔLk relative to CEN4 and compared with the experimental data (green).

centromeres was not established by protein interactions bridging CDEI and CDEIII.

We examined finally whether CDEII, which is essential for centromere function along with CDEIII, was required to determine the topology of DNA at the point centromere. For this purpose, we replaced the AT-rich CDEII sequence of *CEN4* in the 1,286-bp minichromosomes by a corresponding segment of *High2*, which is not AT rich (55% GC). We did the same replacement in the *ΔCDEI* construct, such that only the CDEIII element was conserved in the insert (Figures 5A and S5). The resulting *ΔCDEII* and *ΔCDEI+II* minichromosomes presented low mitotic stability and were recovered as high-copy episomes, which corroborated the loss of centromere function. Both *ΔCDEII* and *ΔCDEI+II* minichromosomes presented similar DNA topology as they had a *ΔLk* of −6.9 and −7.0, respectively (Figures 5B and 5C). These *ΔLk* values indicated that the inserts with *ΔCDEII* and *ΔCDEI+II* do not produce the gain of +0.6 *Lk* units observed with the full *CEN4* sequence. Therefore, both CDEIII and CDEII are necessary to establish the topology of DNA at the point centromere.

DISCUSSION

Here, we have shown that the point centromere of budding yeast stabilizes a *ΔLk* of +0.6 units and that this topology is determined by the protein complexes bound to CDEII and/or CDEIII, but not to CDEI. To reach these conclusions, we excluded other plausible mechanisms that could account for the *Lk* differences between centromeric and non-centromeric constructs. First, we eliminated plausible alterations of *Lk* values during cell disruption and DNA extraction. We found that changes in temperature during sample manipulation markedly deviate the *Lk* of yeast minichromosomes. Thus, we fixed the in vivo *ΔLk* values by quenching the yeast cultures with a procedure that irreversibly inactivates the cellular topoisomerases. Second, we solubilized the minichromosomes and incubated them with topoisomerases at the same temperature as that used for the cultures in order to discern whether in vivo *ΔLk* values were constrained by chromatin structure or were relaxable as free DNA supercoils. Third, in addition to comparing the *Lk* distributions of distinct minichromosomes directly as in previous studies (Bloom et al., 1983, 1984; Furuyama and Henikoff, 2009), we determined the Δ*Lk* of each minichromosome using *Lk*° as a reference value and then compared the Δ*Lk* of different minichromosomes. To calculate Δ*Lk* accurately, we obtained *Lk*° by relaxing DNA circles of the same length and at the same temperature as used for the in vivo minichromosomes. Only using this Δ*Lk* approach could we determine unambiguously the individual contribution (*Lk* gain) of the elements that we inserted or deleted from the minichromosomes. In this regard, our experimental data show that the TA1 minichromosome constraints *ΔLk* = −9.4. This measurement corrects the *ΔLk* approximately −7 of TA1 reported in earlier studies, in which Δ*Lk* was determined relative to the gel-position nicked circles instead from *Lk*° (Pederson et al., 1986). Since the TA1 minichromosome accommodates seven nucleosomes and the average value of *ΔLk* stabilized by nucleosomes is −1 (Prunell, 1998), it is possible that other protein-DNA complexes or high-order folding of chromatin may contribute additional changes to the *Lk* of the minichromosome in vivo. In addition,

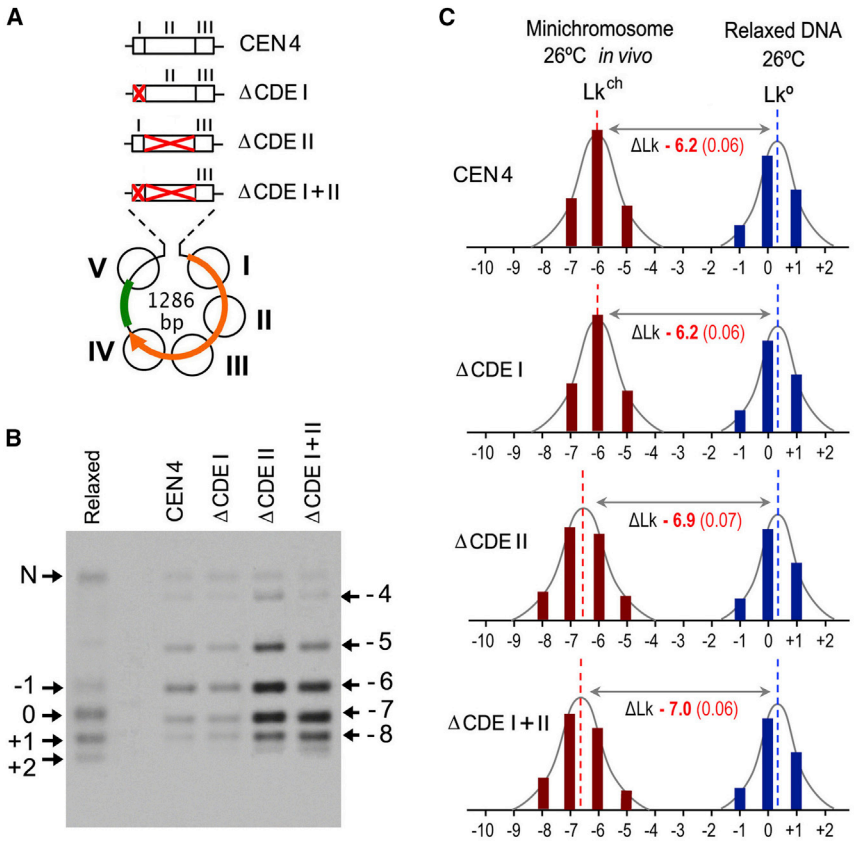

Figure 5. Effect of the Disruption of CDEI and CDEII on the Topology of DNA at Point Centromeres

(A) Structure and *Lk* distributions of 1,286-bp minichromosomes that carried *CEN4* and *CEN4* with CDEI disrupted (ΔCDEI), CDEII disrupted (ΔCDEII), and both CDEI and CDEII disrupted (ΔCDEI+II). See Figure S5 for details.

(B) *Lk* distributions of the above 1,286-bp minichromosomes and of relaxed DNA of the same length. Electrophoresis and counting of individual topoisomers was done as in Figure 3C.

(C) Aligned histograms of the *Lk* distributions of relaxed DNA circles and of the 1,286-bp minichromosomes that carried *CEN4*, ΔCDEI, ΔCDEII, and ΔCDEI+II. *ΔLk* values were calculated as in Figure 1D. Average values (±SD) of three independent experiments are indicated.

given that nucleosomes are more dynamic and structurally heterogeneous than initially assumed (Zlatanova et al., 2009; Rhee et al., 2014), it is also plausible that not all nucleosomes or nucleosome-like particles produce the same *ΔLk* values in vivo. Some complexes may induce $\Delta Lk < -1$, while others may do the opposite (as it is the case of point centromeres). Following our approach, we show that the insertion of a point centromere produces always a gain of +0.6 *Lk* units, whereas an insert containing the sequence of a stable nucleosome (*High2*) and the *mutCEN* sequence produce gains of −1.4 and −1.2 *Lk* units, respectively. Our results are thus consistent with the difference of about +2 *Lk* units between centromeric and non-centromeric minichromosomes observed in previous studies (Bloom et al., 1983, 1984; Furuyama and Henikoff, 2009). Finally, we discarded that the gain of +0.6 *ΔLk* units produced by a point centromere is due to alterations of DNA topology induced in the neighboring regions. We show that by reducing the size of the minichromosomes and the inserted sequences, there is no dysfunction of the adjacent TRP and ARS elements as long as the CDEs are flanked by minimum linker segments and that this proximity does not induce loss of nucleosomes adjacent to point centromeres. These observations are consistent with previous studies showing that the native yeast point centromeres are generally flanked by regularly spaced nucleosomes (Bloom and Carbon, 1982; Hsu et al., 2003: Furuyama and Biggins, 2007; Gkikopoulos et al., 2011; Cole et al., 2011). Therefore, the stabilization of +0.6 *ΔLk* units is an intrinsic trait of the point centromere architecture.

Next, we have shown that the stabilization of +0.6 *Lk* units by the point centromere is independent of the variable length of CDEII and thus the rotational phasing between CDEI and CDEIII. This finding argues against the existence of tight interactions between cbf1 and CBF3 that determine the topology of the DNA (Hemmerich et al., 2000; Xiao et al., 2011; Cho and Harrison, 2011). We corroborated this conclusion by showing that CDEI mutations that abolish Cbf1 binding (Wilmen et al., 1994) also have no effect on the DNA topology. This observation was surprising, because Cbf1 induces a strong bend (~70°) in CDEI (Niedenthal et al., 1993). Therefore, given that CDEI is not essential for centromere activity, we conclude that the CDEI-cbf1 complex and its induced bend are irrelevant in defining the essential topology of the point centromere. In contrast, we have shown that the stabilization of the +0.6 *Lk* units depends on both the CDEII and CDEIII segments. Disruption of CDEII abolishes the stabilization of the +0.6 *Lk* units, even though CBF3 may still bind to CDEIII. Disruption of CDEIII (*mutCEN*) produces a $\Delta\Delta Lk$ of −1.2 *Lk* units, which suggests the assembly of a conventional nucleosome in the place of the point centromere.

The protein complexes that interact with CDEII and CDEIII may alter the twist (*Tw*) and the writhe (*Wr*) of DNA. *Tw* computes the winding of each strand around the DNA axis, and *Wr* measures the non-planar turns of the DNA axis. Since $\Delta Lk = \Delta Tw + \Delta Wr$, stabilization of +0.6 *Lk* units could result from over-twisting ($\Delta Tw > 0$) and/or right-handed turning ($\Delta Wr > 0$) of the CDEII and/or CDEIII segments. This scenario suggests that left-handed wrapping of DNA ($\Delta Wr < 0$), as occurs in conventional nucleosomes, is not likely to happen at point centromeres. In such a case, CDEII and CDEIII would have to be severely over-twisted (e.g., DNA helical repeat of ~9 bp instead of 10.5 bp) in order to neutralize the negative *Wr* of DNA and constrain additional +0.6 *Lk* units. A more bearable situation would be that DNA does not turn or describes a flat U-turn at the point

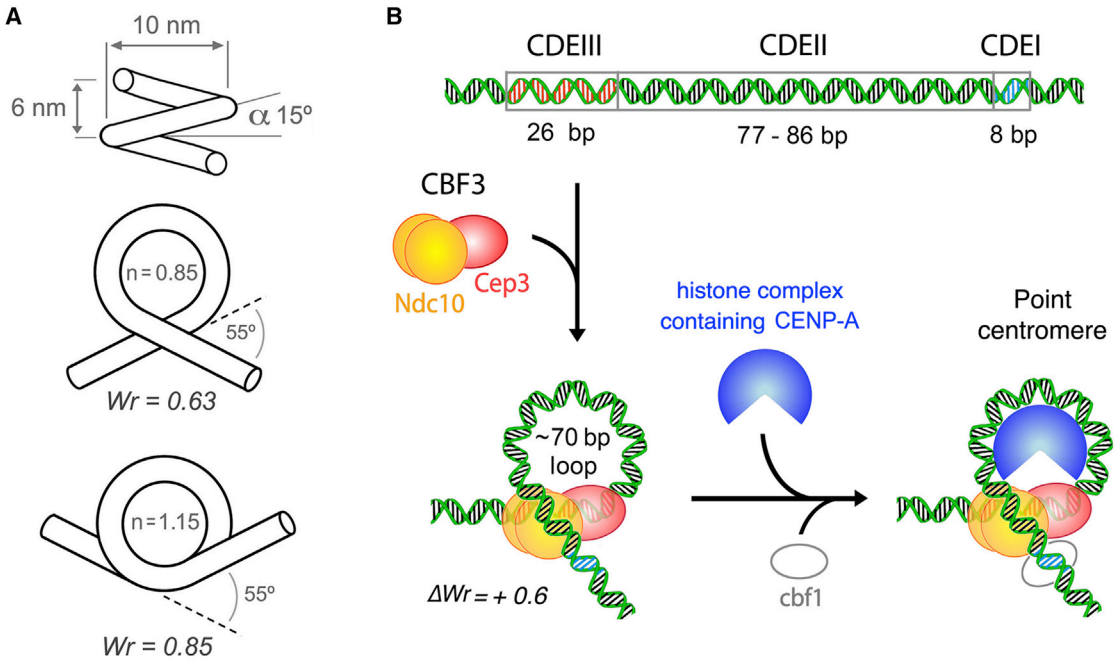

Figure 6. Model of DNA Topology and Global Architecture of the Yeast Point Centromere

(A) DNA writhe (*Wr*) of a right-handed coil that has pitch angle (α) of 15° and completes 0.85 or 1.15 helical turns (*n*). Angle α corresponds to a diameter/pitch ratio of 10/6 (diameter of nucleosomal DNA ~10 nm, DNA binding site separation in Ndc10 ~6 nm). Values of *n* (0.85 and 1.15) correspond to turns of 360° ± 55°. *Wr* is calculated following Fuller (1971) as $n\ (1 - \sin \alpha)$.

(B) Plausible assembly and architecture of a point centromere that constrains a ΔLk approximately +0.6. CDEIII is occupied by the CBF3 complex, in which the Cep3 homodimer (red) interacts with ~15 bp of the DNA, and one subunit of the Ndc10 homodimer (yellow) binds ~10 bp of DNA next to Cep3. For clarity, the Skp1-Ctf13 heterodimer of CBF3 is not shown. The second subunit of Ndc10 then interacts with a looped DNA segment in CDEII ~70 bp apart. This loop conforms a right-handed turn of dimensions $n = 0.85$ and $\alpha = 15°$, such that its *Wr* is +0.6.

A histone complex that contains CENP-A is then recruited by CBF3 and accommodated in the looped DNA. The interaction of cbf1 with CDEI stabilizes the full complex but does not alter its DNA topology.

centromere, such that its *Wr* ~0. In this case, DNA over-twisting across CDEII and CDEIII could suffice to constrain +0.6 *Lk* units. However, the simplest explanation for the stabilization of +0.6 *Lk* units is that DNA is wrapped in a right-handed manner at the point centromere ($\Delta Wr > 0$), as proposed in previous reports (Furuyama et al., 2006; Furuyama and Henikoff, 2009). This right-handed path could be determined by the CENP-A histone complex that is recruited by CBF3. However, there is no experimental evidence of inherently right-handed histone complexes. Moreover, $(CENP\text{-}A/H4/H2B/H2A)_2$ octamers assembled in vitro are left-handed (Sekulic et al., 2010; Tachiwana et al., 2011). This octamer configuration does not exclude that the horseshoe shape of sub-octameric particles containing CENP-A (tetrasomes or hemisomes) have the flexibility to accommodate DNA in a right- or left-handed path. This property is akin to $(H3/H4)_2$ tetrasomes, which can shift their chirality in function of the DNA supercoiling state (Hamiche et al., 1996) and by spontaneous fluctuations during nucleosome assembly (Vlijm et al., 2015). Then, in the case of the point centromere, the path of the DNA may be followed but not determined by histone-DNA interactions. Our results support a model in which a right-handed turn of DNA is determined by the CBF3 complex.

The assembly of the CBF3 complex is highly regulated and occurs prior to binding to DNA (Lechner and Carbon, 1991; Russell et al., 1999). CBF3 recognizes the CDEIII sequence via the Cep3 dimer, which contacts ~15 bp of CDEIII, including the essential CCG motif (Espelin et al., 1997; Pietrasanta et al., 1999; Russell et al., 1999; Purvis and Singleton, 2008). In contrast, the Ndc10 dimer of CBF3 does not recognize a specific DNA sequence. Ndc10 interacts with DNA inside and outside CDEIII, and also with CDEII, as it shows preferential binding to AT-rich regions (Espelin et al., 1997, 2003). These extended interactions initially suggested that several Ndc10 dimers concur in the point centromere. However, structural data revealed that the Ndc10 dimer binds two separate segments of DNA, each of ~10 bp (Cho and Harrison, 2012). Thus, while one subunit of Ndc10 binds DNA in defined register next to Cep3, the other subunit can interact with other DNA molecules or with a looped DNA segment located near CDEIII. Remarkably, this looping capacity was observed in earlier AFM studies of CBF3 bound to DNA (Pietrasanta et al., 1999). Specifically, the CBF3 complex shortened the DNA by ~70 bp and rendered an angle of 55° between the entry and exit segments of DNA. Thus, we calculated the theoretical *Wr* of a right-handed loop of 70 bp anchored by an Ndc10 dimer (Figure 6A). For a simple helix, $Wr = n\ (1 - \sin \alpha)$, *n* being the number of helical turns and α the angle of the helical pitch (Fuller, 1971). As the entry and exit DNA segments in the CBF3 complexes observed by AFM

formed an angle of 55°, we considered two plausible n values: n = 1.15 for a turn of 360° + 55°, and n = 0.85 for a turn of 360°–55°. To determine the helical pitch, we considered that the superhelical turn was 6 nm high, which is the approximate DNA-binding site separation in Ndc10 (Cho and Harrison, 2012), and that the turn had a diameter of 10 nm, as for DNA wrapped on a histone core. This geometry produced $\alpha \sim 15°$. Then, for n = 1.15, Wr = 0.84; and for n = 0.85, Wr = 0.63. Remarkably, the latter Wr value would account for the stabilization of ΔLk +0.6 without requiring significant alterations of Tw. Accordingly, we constructed a model of the point centromere in which the Ndc10 dimer configures a right-handed DNA turn (n = 0.85) by anchoring an entry segment at CDEIII (next to Cep3) and an exit segment at CDEII (Figure 6B). This configuration produces a loop of >70 bp, which could accommodate the CENP-A histone complex that is recruited via Scm3 (a CENP-A chaperone recognized by Ndc10) (Cho and Harrison, 2011; Wisniewski et al., 2014). Interestingly, the histone complex that interacts with CDEII elements in vivo has been found in variable bp registers (two orientations and two helical frames one turn apart) (Henikoff et al., 2014). This observation supports that this complex is accommodating into a predefined loop of DNA, rather than occupying a position determined by the DNA sequence. Our model is also consistent with the reported nuclease-protection data, which showed that point centromeres protect tightly a region of 120–135 bp (Cole et al., 2011; Krassovsky et al., 2012). Finally, since CDEI is located outside the looped DNA, our model explains why CDEI and plausible interactions of cbf1 with CBF3 are not relevant in determining the topology of DNA at the point centromere.

The singular topology of DNA constrained by point centromeres may not be an exclusive trait of yeast centromeric chromatin. The stabilization of positive supercoils has been observed in vitro when DNA is mixed with CENP-A/H4/H2B/H2A and the histone chaperone RbAp48 from *Drosophila* (Furuyama and Henikoff, 2009) and when chromatin is assembled with heterotypic histone-like CENP-S/T/W/X tetramers (Takeuchi et al., 2014). The partitioning locus of the yeast 2-μm plasmid, which includes a CENP-A complex, induces also the stabilization of positive supercoils (Huang et al., 2011). Thus, positive supercoiling of DNA may be a general feature of centromeric chromatin, regardless of the rapid evolution of centromeric proteins (Malik and Henikoff, 2009). Left-handed wrapping of DNA in conventional nucleosomes confine DNA unwinding energy and allow specific structural transitions in response to the twisting and pulling forces generated by RNA and DNA polymerases. Centromeres undergo other mechanical processes. Right-handed wrapping of DNA in centromeric chromatin may serve to establish the bipolar orientation of the sister chromatids and to trigger distinctive structural transitions and checkpoint signals in response to the forces generated by the spindle.

EXPERIMENTAL PROCEDURES

Construction of Circular Minichromosomes

The yeast circular minichromosome TA1 (1,453 bp) and its derivatives of 1,686 bp and 1,286 bp were constructed as detailed in Supplemental Experimental Procedures. Oligonucleotides used to produce inserts are described in Table S1, and detailed maps of the insert regions are illustrated in Figures S4 and S5. Linear fragments of each construct were circularized with T4 DNA ligase. Monomeric circles were gel-purified and used to transform the *S. cerevisiae* strain FY251.

Yeast Culture and DNA Extraction of Fixed Minichromosomes

Yeast colonies transformed with TA1-derived minichromosomes were grown at 26°C in standard yeast synthetic media containing TRP dropout supplement (Sigma) and 2% glucose. When the liquid cultures (20 ml) reached mid-log phase (optical density [OD] ~0.8), yeast cells were fixed in vivo by quickly mixing the cultures with one cold volume (−20°C) of ETol solution (95% ethanol, 28 mM toluene, 20 mM Tris HCl [pH 8.8], and 5 mM EDTA). As this fixation precludes the alteration of the in vivo Lk^{ch} values in subsequent manipulations (see Figure S2), the following steps were done at room temperature. Cells were sedimented, washed twice with water, resuspended in 400 μl TE, and transferred to a 1.5-ml microfuge tube containing 400 μl phenol and 400 μl acid-washed glass beads (425–600 μm, Sigma). Mechanic lysis of >80% cells was achieved by shaking the tubes in a FastPrep apparatus for 10 s at power 5. The aqueous phase of the lysed cell suspension was collected, extracted with chloroform, precipitated with ethanol, and resupended in 100 μl Tris-EDTA buffer containing RNase-A. Following 15 min of incubation at 37°, the samples were extracted with phenol and chloroform, precipitated with ethanol, and resupended in 30 μl of TE.

Solubilization of Native Minichromosomes

Yeast liquid cultures (20 ml) at mid-log phase (OD ~0.8) were not fixed with ETol solution. The cells were sedimented, washed with water, and resuspended in 500 μl cold (4°C) buffer L (10 mM Tris-HCl [pH 8], 1 mM EDTA, 1 mM EGTA, 1 mM DTT, 150 mM NaCl, Triton 0.1%, 1 mg/ml pepstatin, 1 mg/ml leupeptin, and 1 mM PMSF). The suspension was transferred to a 1.5-ml microfuge tube containing 500 μl acid-washed glass beads (425–600 μm, Sigma). Mechanic lysis of >80% cells was achieved after six cycles of 30 s of vortexing plus 30 s of ice cooling. The supernatant of the lysate was recovered by centrifugation (2,000 × *g* at 4°C) and loaded on a Sephacryl S-300 column equilibrated with buffer L. Circular minichromosomes eluted in the first filtration volume were adjusted to 8 mM $MgCl_2$ and 1mM ATP, pre-incubated at 26°C for 5 min, and then supplemented with control plasmids and catalytic amounts of purified topoisomerase I of vaccinia virus (Shuman et al., 1988) or *S. cerevisiae* topoisomerase II (Worland and Wang, 1989). Following incubations at 26°C for 10 min, reactions were quenched with one volume of 20 mM EDTA, 0.5% SDS, and 100 mg/ml proteinase K and incubated for 30 min at 60°C. The mixtures were extracted with phenol and chloroform, DNA precipitated with ethanol, and resupended in 30 μl TE.

Indirect End-Labeling of the Micrococcal Nuclease-Digested Chromatin

Circular minichromosomes were solubilized and eluted from a Sephacryl S-300 column as described above and adjusted to 2 mM $CaCl_2$. Following pre-incubation at 25°C for 5 min, micrococcal nuclease was added (2–100 U/ml) and digestions proceeded at 25°C for 5 min. Reactions were quenched with one volume of 20 mM EDTA, 0.5% SDS, 100 mg/ml proteinase K, and incubated for 60 min at 60°C. The mixtures were extracted with phenol and chloroform, DNA precipitated with ethanol and resupended in 30 μl of TE. Digested DNA samples were singly cut with a restriction endonuclease, separated on a agarose gel, blotted, and probed with a short DNA sequence (<200 bp) contiguous to the single restriction site.

Electrophoresis of DNA Topoisomers

DNA extracted from yeast circular minichromosomes (samples of non-centromeric minichromosomes were diluted ~10-fold) and the corresponding DNA circles relaxed in vitro with topoisomerase I at 26°C (temperature at which DNA topology was fixed in vivo) were loaded onto 1.2% (w/v) agarose gels. One-dimensional electrophoresis was carried out at 2.5 V/cm for 18 hr in Tris-borate EDTA (TBE) buffer (89 mM Tris-borate and 2 mM EDTA) containing 0.2 μg/ml chloroquine. Two-dimensional electrophoresis was in TBE containing 0.1 or 0.2 μg/ml chloroquine in the first dimension (2.5 V/cm for 18 hr) and in

TBE containing 1 μg/ml chloroquine in the second dimension (5 V/cm for 4 hr). Gel-markers of *Lk* topoisomers were obtained by mixing partially relaxed samples of supercoiled DNA rings. Gels were blot-transferred to a nylon membrane and probed at 60°C with the 1,453-bp TRP1ARS1 sequence labeled with AlkPhos Direct (GE Healthcare). Chemiluminescent signals of increasing exposition periods were recorded on X-ray films.

DNA Topology Analyses

The midpoint of each *Lk* distribution, which does not necessarily coincide with the gel position of main topoisomers, was determined by quantifying with the ImageJ software the relative intensity of non-saturated signals of the individual *Lk* topoisomers. *ΔLk* was calculated as the distance (*Lk* units) between the midpoints of minichromosome (Lk^{ch}) and relaxed DNA (Lk°) distributions, being both *Lk* distributions produced at the same temperature and resolved in the same gel electrophoresis.

SUPPLEMENTAL INFORMATION

Supplemental information includes Supplemental Experimental Procedures, five figures, and one table and can be found with this article online at http://dx.doi.org/10.1016/j.celrep.2015.09.039.

AUTHOR CONTRIBUTIONS

O.D.-I. and J.R. conceived the research, designed experiments, and analyzed data. O.D.-I., B.M.-G., J.S., and A.V. prepared materials and conducted experiments. J.R. wrote the manuscript.

ACKNOWLEDGMENTS

This research was supported by the Plan Nacional de I+D+I of Spain (grant BFU2011-23851 to J.R.).

Received: April 17, 2015
Revised: August 8, 2015
Accepted: September 14, 2015
Published: October 15, 2015

REFERENCES

Aravamudhan, P., Felzer-Kim, I., and Joglekar, A.P. (2013). The budding yeast point centromere associates with two Cse4 molecules during mitosis. Curr. Biol. *23*, 770–774.

Baker, R.E., Fitzgerald-Hayes, M., and O'Brien, T.C. (1989). Purification of the yeast centromere binding protein CP1 and a mutational analysis of its binding site. J. Biol. Chem. *264*, 10843–10850.

Biggins, S. (2013). The composition, functions, and regulation of the budding yeast kinetochore. Genetics *194*, 817–846.

Black, B.E., Jansen, L.E., Foltz, D.R., and Cleveland, D.W. (2010). Centromere identity, function, and epigenetic propagation across cell divisions. Cold Spring Harb. Symp. Quant. Biol. *75*, 403–418.

Bloom, K.S. (2014). Centromeric heterochromatin: the primordial segregation machine. Annu. Rev. Genet. *48*, 457–484.

Bloom, K.S., and Carbon, J. (1982). Yeast centromere DNA is in a unique and highly ordered structure in chromosomes and small circular minichromosomes. Cell *29*, 305–317.

Bloom, K.S., Fitzgerald-Hayes, M., and Carbon, J. (1983). Structural analysis and sequence organization of yeast centromeres. Cold Spring Harb. Symp. Quant. Biol. *47*, 1175–1185.

Bloom, K., Amaya, E., and Yeh, E. (1984). Centromeric DNA structure in yeast chromatin. In Molecular Biology of the Cytoskeleton, G.G. Borisy, D.W. Cleveland, and D.B. Murphy, eds. (Cold Spring Harbor Laboratory Press), pp. 175–184.

Bui, M., Dimitriadis, E.K., Hoischen, C., An, E., Quénet, D., Giebe, S., Nita-Lazar, A., Diekmann, S., and Dalal, Y. (2012). Cell-cycle-dependent structural transitions in the human CENP-A nucleosome in vivo. Cell *150*, 317–326.

Burrack, L.S., and Berman, J. (2012). Neocentromeres and epigenetically inherited features of centromeres. Chromosome Res. *20*, 607–619.

Cai, M.J., and Davis, R.W. (1989). Purification of a yeast centromere-binding protein that is able to distinguish single base-pair mutations in its recognition site. Mol. Cell. Biol. *9*, 2544–2550.

Camahort, R., Shivaraju, M., Mattingly, M., Li, B., Nakanishi, S., Zhu, D., Shilatifard, A., Workman, J.L., and Gerton, J.L. (2009). Cse4 is part of an octameric nucleosome in budding yeast. Mol. Cell *35*, 794–805.

Cho, U.S., and Harrison, S.C. (2011). Recognition of the centromere-specific histone Cse4 by the chaperone Scm3. Proc. Natl. Acad. Sci. USA *108*, 9367–9371.

Cho, U.S., and Harrison, S.C. (2012). Ndc10 is a platform for inner kinetochore assembly in budding yeast. Nat. Struct. Mol. Biol. *19*, 48–55.

Clarke, L. (1998). Centromeres: proteins, protein complexes, and repeated domains at centromeres of simple eukaryotes. Curr. Opin. Genet. Dev. *8*, 212–218.

Cole, H.A., Howard, B.H., and Clark, D.J. (2011). The centromeric nucleosome of budding yeast is perfectly positioned and covers the entire centromere. Proc. Natl. Acad. Sci. USA *108*, 12687–12692.

Connelly, C., and Hieter, P. (1996). Budding yeast SKP1 encodes an evolutionarily conserved kinetochore protein required for cell cycle progression. Cell *86*, 275–285.

Dalal, Y., Wang, H., Lindsay, S., and Henikoff, S. (2007). Tetrameric structure of centromeric nucleosomes in interphase Drosophila cells. PLoS Biol. *5*, e218.

Depew, D.E., and Wang, J.C. (1975). Conformational fluctuations of DNA helix. Proc. Natl. Acad. Sci. USA *72*, 4275–4279.

Dimitriadis, E.K., Weber, C., Gill, R.K., Diekmann, S., and Dalal, Y. (2010). Tetrameric organization of vertebrate centromeric nucleosomes. Proc. Natl. Acad. Sci. USA *107*, 20317–20322.

Espelin, C.W., Kaplan, K.B., and Sorger, P.K. (1997). Probing the architecture of a simple kinetochore using DNA-protein crosslinking. J. Cell Biol. *139*, 1383–1396.

Espelin, C.W., Simons, K.T., Harrison, S.C., and Sorger, P.K. (2003). Binding of the essential Saccharomyces cerevisiae kinetochore protein Ndc10p to CDEII. Mol. Biol. Cell *14*, 4557–4568.

Fuller, F.B. (1971). The writhing number of a space curve. Proc. Natl. Acad. Sci. USA *68*, 815–819.

Furuyama, S., and Biggins, S. (2007). Centromere identity is specified by a single centromeric nucleosome in budding yeast. Proc. Natl. Acad. Sci. USA *104*, 14706–14711.

Furuyama, T., and Henikoff, S. (2009). Centromeric nucleosomes induce positive DNA supercoils. Cell *138*, 104–113.

Furuyama, T., Dalal, Y., and Henikoff, S. (2006). Chaperone-mediated assembly of centromeric chromatin in vitro. Proc. Natl. Acad. Sci. USA *103*, 6172–6177.

Furuyama, T., Codomo, C.A., and Henikoff, S. (2013). Reconstitution of hemisomes on budding yeast centromeric DNA. Nucleic Acids Res. *41*, 5769–5783.

Gkikopoulos, T., Singh, V., Tsui, K., Awad, S., Renshaw, M.J., Scholfield, P., Barton, G.J., Nislow, C., Tanaka, T.U., and Owen-Hughes, T. (2011). The SWI/SNF complex acts to constrain distribution of the centromeric histone variant Cse4. EMBO J. *30*, 1919–1927.

Haase, J., Mishra, P.K., Stephens, A., Haggerty, R., Quammen, C., Taylor, R.M., 2nd, Yeh, E., Basrai, M.A., and Bloom, K. (2013). A 3D map of the yeast kinetochore reveals the presence of core and accessory centromere-specific histone. Curr. Biol. *23*, 1939–1944.

Hamiche, A., Carot, V., Alilat, M., De Lucia, F., O'Donohue, M.F., Revet, B., and Prunell, A. (1996). Interaction of the histone (H3-H4)2 tetramer of the nucleosome with positively supercoiled DNA minicircles: Potential flipping of the

protein from a left- to a right-handed superhelical form. Proc. Natl. Acad. Sci. USA *93*, 7588–7593.

Hemmerich, P., Stoyan, T., Wieland, G., Koch, M., Lechner, J., and Diekmann, S. (2000). Interaction of yeast kinetochore proteins with centromere-protein/transcription factor Cbf1. Proc. Natl. Acad. Sci. USA *97*, 12583–12588.

Henikoff, S., and Furuyama, T. (2010). Epigenetic inheritance of centromeres. Cold Spring Harb. Symp. Quant. Biol. *75*, 51–60.

Henikoff, S., and Furuyama, T. (2012). The unconventional structure of centromeric nucleosomes. Chromosoma *121*, 341–352.

Henikoff, S., Ramachandran, S., Krassovsky, K., Bryson, T.D., Codomo, C.A., Brogaard, K., Widom, J., Wang, J.P., and Henikoff, J.G. (2014). The budding yeast Centromere DNA Element II wraps a stable Cse4 hemisome in either orientation in vivo. eLife *3*, e01861.

Hsu, J.M., Huang, J., Meluh, P.B., and Laurent, B.C. (2003). The yeast RSC chromatin-remodeling complex is required for kinetochore function in chromosome segregation. Mol. Cell. Biol. *23*, 3202–3215.

Huang, C.C., Chang, K.M., Cui, H., and Jayaram, M. (2011). Histone H3-variant Cse4-induced positive DNA supercoiling in the yeast plasmid has implications for a plasmid origin of a chromosome centromere. Proc. Natl. Acad. Sci. USA *108*, 13671–13676.

Jehn, B., Niedenthal, R., and Hegemann, J.H. (1991). In vivo analysis of the Saccharomyces cerevisiae centromere CDEIII sequence: requirements for mitotic chromosome segregation. Mol. Cell. Biol. *11*, 5212–5221.

Jiang, C., and Pugh, B.F. (2009). A compiled and systematic reference map of nucleosome positions across the Saccharomyces cerevisiae genome. Genome Biol. *10*, R109.

Jiang, W., Lechner, J., and Carbon, J. (1993). Isolation and characterization of a gene (CBF2) specifying a protein component of the budding yeast kinetochore. J. Cell Biol. *121*, 513–519.

Krassovsky, K., Henikoff, J.G., and Henikoff, S. (2012). Tripartite organization of centromeric chromatin in budding yeast. Proc. Natl. Acad. Sci. USA *109*, 243–248.

Lechner, J., and Carbon, J. (1991). A 240 kd multisubunit protein complex, CBF3, is a major component of the budding yeast centromere. Cell *64*, 717–725.

Lochmann, B., and Ivanov, D. (2012). Histone H3 localizes to the centromeric DNA in budding yeast. PLoS Genet. *8*, e1002739.

Malik, H.S., and Henikoff, S. (2009). Major evolutionary transitions in centromere complexity. Cell *138*, 1067–1082.

Miell, M.D., Fuller, C.J., Guse, A., Barysz, H.M., Downes, A., Owen-Hughes, T., Rappsilber, J., Straight, A.F., and Allshire, R.C. (2013). CENP-A confers a reduction in height on octameric nucleosomes. Nat. Struct. Mol. Biol. *20*, 763–765.

Mishra, P.K., Ottmann, A.R., and Basrai, M.A. (2013). Structural integrity of centromeric chromatin and faithful chromosome segregation requires Pat1. Genetics *195*, 369–379.

Mizuguchi, G., Xiao, H., Wisniewski, J., Smith, M.M., and Wu, C. (2007). Nonhistone Scm3 and histones CenH3-H4 assemble the core of centromere-specific nucleosomes. Cell *129*, 1153–1164.

Niedenthal, R.K., Sen-Gupta, M., Wilmen, A., and Hegemann, J.H. (1993). Cpf1 protein induced bending of yeast centromere DNA element I. Nucleic Acids Res. *21*, 4726–4733.

Padeganeh, A., Ryan, J., Boisvert, J., Ladouceur, A.M., Dorn, J.F., and Maddox, P.S. (2013). Octameric CENP-A nucleosomes are present at human centromeres throughout the cell cycle. Curr. Biol. *23*, 764–769.

Pederson, D.S., Venkatesan, M., Thoma, F., and Simpson, R.T. (1986). Isolation of an episomal yeast gene and replication origin as chromatin. Proc. Natl. Acad. Sci. USA *83*, 7206–7210.

Pietrasanta, L.I., Thrower, D., Hsieh, W., Rao, S., Stemmann, O., Lechner, J., Carbon, J., and Hansma, H. (1999). Probing the Saccharomyces cerevisiae centromeric DNA (CEN DNA)-binding factor 3 (CBF3) kinetochore complex by using atomic force microscopy. Proc. Natl. Acad. Sci. USA *96*, 3757–3762.

Prunell, A. (1998). A topological approach to nucleosome structure and dynamics: the linking number paradox and other issues. Biophys. J. *74*, 2531–2544.

Purvis, A., and Singleton, M.R. (2008). Insights into kinetochore-DNA interactions from the structure of Cep3Delta. EMBO Rep. *9*, 56–62.

Rhee, H.S., Bataille, A.R., Zhang, L., and Pugh, B.F. (2014). Subnucleosomal structures and nucleosome asymmetry across a genome. Cell *159*, 1377–1388.

Russell, I.D., Grancell, A.S., and Sorger, P.K. (1999). The unstable F-box protein p58-Ctf13 forms the structural core of the CBF3 kinetochore complex. J. Cell Biol. *145*, 933–950.

Schueler, M.G., and Sullivan, B.A. (2006). Structural and functional dynamics of human centromeric chromatin. Annu. Rev. Genomics Hum. Genet. *7*, 301–313.

Segal, E., Fondufe-Mittendorf, Y., Chen, L., Thåström, A., Field, Y., Moore, I.K., Wang, J.P., and Widom, J. (2006). A genomic code for nucleosome positioning. Nature *442*, 772–778.

Sekulic, N., Bassett, E.A., Rogers, D.J., and Black, B.E. (2010). The structure of (CENP-A-H4)(2) reveals physical features that mark centromeres. Nature *467*, 347–351.

Shuman, S., Golder, M., and Moss, B. (1988). Characterization of vaccinia virus DNA topoisomerase I expressed in Escherichia coli. J. Biol. Chem. *263*, 16401–16407.

Tachiwana, H., Kagawa, W., Shiga, T., Osakabe, A., Miya, Y., Saito, K., Hayashi-Takanaka, Y., Oda, T., Sato, M., Park, S.Y., et al. (2011). Crystal structure of the human centromeric nucleosome containing CENP-A. Nature *476*, 232–235.

Takeuchi, K., Nishino, T., Mayanagi, K., Horikoshi, N., Osakabe, A., Tachiwana, H., Hori, T., Kurumizaka, H., and Fukagawa, T. (2014). The centromeric nucleosome-like CENP-T-W-S-X complex induces positive supercoils into DNA. Nucleic Acids Res. *42*, 1644–1655.

Thoma, F., Bergman, L.W., and Simpson, R.T. (1984). Nuclease digestion of circular TRP1ARS1 chromatin reveals positioned nucleosomes separated by nuclease-sensitive regions. J. Mol. Biol. *177*, 715–733.

Vlijm, R., Lee, M., Lipfert, J., Lusser, A., Dekker, C., and Dekker, N.H. (2015). Nucleosome assembly dynamics involve spontaneous fluctuations in the handedness of tetrasomes. Cell Rep. *10*, 216–225.

Wilmen, A., Pick, H., Niedenthal, R.K., Sen-Gupta, M., and Hegemann, J.H. (1994). The yeast centromere CDEI/Cpf1 complex: differences between in vitro binding and in vivo function. Nucleic Acids Res. *22*, 2791–2800.

Wisniewski, J., Hajj, B., Chen, J., Mizuguchi, G., Xiao, H., Wei, D., Dahan, M., and Wu, C. (2014). Imaging the fate of histone Cse4 reveals de novo replacement in S phase and subsequent stable residence at centromeres. eLife *3*, e02203.

Worland, S.T., and Wang, J.C. (1989). Inducible overexpression, purification, and active site mapping of DNA topoisomerase II from the yeast Saccharomyces cerevisiae. J. Biol. Chem. *264*, 4412–4416.

Xiao, H., Mizuguchi, G., Wisniewski, J., Huang, Y., Wei, D., and Wu, C. (2011). Nonhistone Scm3 binds to AT-rich DNA to organize atypical centromeric nucleosome of budding yeast. Mol. Cell *43*, 369–380.

Zhang, W., Colmenares, S.U., and Karpen, G.H. (2012). Assembly of Drosophila centromeric nucleosomes requires CID dimerization. Mol. Cell *45*, 263–269.

Zlatanova, J., Bishop, T.C., Victor, J.M., Jackson, V., and van Holde, K. (2009). The nucleosome family: dynamic and growing. Structure *17*, 160–171.